Entangled coherent states versus entangled photon pairs for practical quantum-information processing

Kimin Park and Hyunseok Jeong*

Center for Macroscopic Quantum Control, Department of Physics and Astronomy, Seoul National University, Seoul 151-742, Korea

(Received 7 July 2010; published 27 December 2010)

We compare effects of decoherence and detection inefficiency on entangled coherent states (ECSs) and entangled photon pairs (EPPs), both of which are known to be particularly useful for quantum-information processing (QIP). When decoherence effects caused by photon losses are heavy, the ECSs outperform the EPPs as quantum channels for teleportation both in fidelities and in success probabilities. On the other hand, when inefficient detectors are used, the teleportation scheme using the ECSs suffers undetected errors that result in the degradation of fidelity, while this is not the case for the teleportation scheme using the EPPs. Our study reveals the merits and demerits of the two types of entangled states in realizing practical QIP under realistic conditions.

DOI: 10.1103/PhysRevA.82.062325 PACS number(s): 03.67.Hk, 42.50.Ex, 03.65.Yz

I. INTRODUCTION

All-optical systems have been studied as a prominent candidate for physical implementations of quantum-information processing (QIP) [1,2]. Quantum teleportation, which uses entangled quantum states as quantum channels, plays a crucial role in optical quantum computation and communication [3,4]. One of the most difficult parts in realizing quantum teleportation using optical systems is an efficient realization of the Bell-state measurement, in which four Bell states should be discriminated. It was shown that the four Bell states cannot be discriminated when only linear optical elements are used [5,6], which makes high success probability for quantum teleportation hard to achieve. For example, in the teleportation scheme based on an entangled photon pair (EPP) [7], the success probability of the Bell measurement is bounded by 50% when using only linear optical elements [8]. Even though universal gate operations can be realized based on linear optics and photon detection [3], this type of problem is one of the major hindrances to the implementation of deterministic gate operations, as well as scalable quantum computation.

An alternative qubit-based teleportation scheme was suggested [9,10] using an entangled coherent state (ECS) as the quantum channel. In fact, the ECSs have been found to be useful not only for fundamental tests of quantum theory [11] but also for various applications in QIP [9,10,12–19]. In this approach, a qubit is composed of two coherent states, $|\pm\alpha\rangle$, where $\pm\alpha$ are the coherent amplitudes [20]. It was explicitly pointed out in Refs. [10,14] that all four Bell states in the form of ECSs can be well discriminated using only a beam splitter and two photon-number-resolving detectors. This has become a remarkable advantage in designing quantum computing schemes using coherent-state qubits [13,15] including deterministic gate operations with ECSs as off-line resources [15]. Recently it was shown that fault-tolerant quantum computing may be realized with coherent-state qubits with amplitudes $\alpha > 1.2$ [17].

Implementations of high-fidelity EPPs and ECSs in free-traveling fields are challenging and crucial tasks for optical QIP. Recently, the realization of an electrically driven source of EPPs, consisting of a quantum dot embedded in a semiconductor light-emitting-diode structure, has been reported [21]. Even though the generation of high-fidelity ECSs is a demanding task, remarkable experimental progress has recently been made in generating single-mode superpositions of coherent states [22–24], with which ECSs would easily be produced using an additional beam splitter. Based on such progress, several suggestions for the same purpose but higher fidelities and larger amplitudes [25] have now become closer to the experimental realization. Efforts to generate arbitrary coherent-state qubits are also being made [26]. Another difficult problem in the approach based on ECSs is that photon-number-resolving detectors are required, while ongoing efforts are being made for the development of such detectors [27,28].

It is therefore important to compare the two optical QIP schemes, one with single-photon qubits and EPPs and the other with coherent-state qubits and ECSs, for efficient implementations of QIP in the long term. First, decoherence of quantum channels caused by photon losses may be an obstacle against optical QIP. This would be non-negligible particularly for long-distance quantum communication. We therefore study its effects on the two aforementioned teleportation schemes. In general, when decoherence effect caused by photon losses is heavy (or the decoherence time of the quantum channel is long), the ECSs outperform the EPPs as quantum channels both in teleportation fidelities and in success probabilities. This tendency becomes prominent when the amplitude α is small: The ECSs outperform the EPPs regardless of the decoherence time both in fidelities and in success probabilities for $\alpha \lesssim 0.8$.

We also pay particular attention to the issue of detection inefficiency, which is a crucial detrimental factor in realizing practical QIP within all-optical systems. We point out that when inefficient detectors are used, the teleportation scheme using ECSs suffers undetected errors that result in the degradation of fidelity. This is not the case for the teleportation scheme using EPPs as photon losses right before the detector errors are detected by the absence of the detection signals itself. We then present the results when both of the two factors, decoherence of the channel and detection inefficiency,

*h.jeong37@gmail.com

are applied. Our results based on thorough quantitative analysis provide useful guidelines for the choice of a scheme among well-known ones for practical QIP using optical systems.

II. DECOHERENCE OF ECSS AND EPPS

In this section, we introduce the dynamics of ECSs and EPPs in a zero-temperature dissipative environment. In this situation, photon losses occur that cause the decrease of the average photon number and dephasing of the channels at the same time. We discuss how the degrees of entanglement for the ECSs and EPPs decrease by such decoherence effects.

A. Solutions of master equation

We are interested in ECSs in the form of [29]

$$|\psi_{\rm ECS}^{\pm}\rangle = N_\alpha^{\pm}(|\alpha\rangle_1|-\alpha\rangle_2 \pm |-\alpha\rangle_1|\alpha\rangle_2), \tag{1}$$

where $N_\alpha^{\pm} = 1/\sqrt{2\pm 2e^{-4|\alpha|^2}}$ is the normalization factor. The complex amplitude α is assumed to be real throughout the paper for simplicity without losing generality. We shall call $|\psi_{\rm ECS}^{+}\rangle$ ($|\psi_{\rm ECS}^{-}\rangle$) even (odd) ECS as it contains only even (odd) numbers of photons. We also consider an EPP,

$$|\psi_{\rm EPP}\rangle = \frac{1}{\sqrt{2}}(|H\rangle|V\rangle + |V\rangle|H\rangle), \tag{2}$$

where $|H\rangle$ and $|V\rangle$ refer to horizontal and vertical polarization states, respectively. The relative sign between the vector components of the EPP in Eq. (2) was chosen to be $+1$ for simplicity: This sign does not make any meaningful difference in our study, and this is obviously different from the cases of the ECSs in (1) for which the signs in the middle play important roles. We also note that $|H\rangle$ is equivalent to $|1\rangle|0\rangle$ and $|V\rangle$ to $|0\rangle|1\rangle$ in terms of the dual-rail logic QIP.

The time evolution of density operator ρ under the Born-Markov approximation is given by the master equation [30],

$$\frac{\partial\rho}{\partial\tau} = \hat{J}\rho + \hat{L}\rho, \tag{3}$$

where τ is the interaction time, $\hat{J}\rho = \gamma\sum_i a_i\rho a_i^\dagger$, $\hat{L}\rho = -\sum_i \frac{\gamma}{2}(a_i^\dagger a_i\rho + \rho a_i^\dagger a_i)$, γ is the decay constant, and a_i is the annihilation operator for mode i. The formal solution of Eq. (3) is written as $\rho(\tau) = \exp[(\hat{J}+\hat{L})\tau]\rho(0)$, where $\rho(0)$ is the initial density operator. Assuming a zero-temperature bath, we obtain the density operator of the odd and even ECSs decohered in the vacuum environment as [9,10]

$$\begin{aligned}\rho_{\rm ECS}^{\pm}(\tau) = (N_\alpha^{\pm})^2\{&|t\alpha\rangle_1\langle t\alpha|\otimes|-t\alpha\rangle_2\langle -t\alpha| \\ &+|-t\alpha\rangle_1\langle -t\alpha|\otimes|t\alpha\rangle_2\langle t\alpha| \\ &\pm e^{-4\alpha^2r^2}(|t\alpha\rangle_1\langle -t\alpha|\otimes|-t\alpha\rangle_2\langle t\alpha| + \text{H.c.})\},\end{aligned} \tag{4}$$

where $t = e^{-\gamma\tau/2}$ and superscript $+$ ($-$) corresponds to the even (odd) ECS. We define the normalized time as $r = (1-t^2)^{1/2}$ for later use. In what follows, we use only the *odd* ECSs, which are maximally entangled in the $2\otimes 2$ Hilbert space at time $\tau = 0$, as the quantum channels to teleport coherent-state qubits. As we explain later, the odd ECS shows larger success probabilities of teleportation than the even ECS. The density matrix $\rho_{\rm ECS}^{-}$ expressed in the orthogonal basis set $|\pm\rangle = N_\pm\big(|t\alpha\rangle \pm |-t\alpha\rangle\big)$ is given as

$$\rho_{\rm ECS}^{-}(\tau) = \frac{1}{4(-1+e^{4\alpha^2})}\begin{pmatrix} A & 0 & 0 & D \\ 0 & B & -B & 0 \\ 0 & -B & B & 0 \\ D & 0 & 0 & C \end{pmatrix}, \tag{5}$$

where

$$\begin{aligned} A &= e^{-4(-1+r^2)\alpha^2}(-1+e^{4r^2\alpha^2})(1+e^{2(-1+r^2)\alpha^2})^2, \\ B &= -1+e^{4\alpha^2}-e^{4r^2\alpha^2}+e^{-4(-1+r^2)\alpha^2}, \\ C &= e^{-4(-1+r^2)\alpha^2}(-1+e^{4r^2\alpha^2})(-1+e^{2(-1+r^2)\alpha^2})^2, \\ D &= -1-e^{4\alpha^2}+e^{4r^2\alpha^2}+e^{-4(-1+r^2)\alpha^2}. \end{aligned} \tag{6}$$

Using the same master equation, one can also find the density operator of the EPP for general τ, initially given as $\rho_{\rm EPP}(0) \equiv |\psi_{\rm EPP}\rangle\langle\psi_{\rm EPP}|$ at $\tau = 0$,

$$\begin{aligned}\rho_{\rm EPP}(\tau) = e^{-2\gamma\tau}\rho_{\rm EPP}(0) &- 2(e^{-2\gamma\tau}-e^{-\gamma\tau})\rho_1 \\ &+ (e^{-2\gamma\tau}-2e^{-\gamma\tau}+1)\,\rho_v,\end{aligned} \tag{7}$$

where $\rho_1 = \frac{1}{4}\sum_{i=1}^4 |1\rangle_i\langle 1|$ is a mixed single-photon-state density matrix, $|1\rangle_i \equiv |0\rangle\ldots|1\rangle_i\ldots|0\rangle$ is a shorthand notation for a single photon occupying mode i and the vacuum in all other modes, and ρ_v represents the vacuum state for every mode. The density matrix can be represented in a basis set of $|H\rangle$, $|V\rangle$, and $|0\rangle$ similarly as before. As one may expect, in a rough sense, the initial entangled two-photon state decays to a mixed single-photon state and then eventually to the vacuum state.

B. Degrees of entanglement

As quantum teleportation utilizes entanglement as a resource, we first consider the dynamics of entanglement for the ECSs and EPPs. Separability of a bipartite system is equivalent to the positivity of the partial transpose of the density matrix when the dimension of the entire system does not exceed six [31,32]. We consider the ECSs in a $2\otimes 2$ Hilbert space (using the dynamic qubit basis), as explained earlier even under the effect of photon losses. On the other hand, the EPPs evolve into $3\otimes 3$ systems due to the addition of the vacuum element under photon loss effects. However, in our case of Eq. (7), negativity of the total density operator equals the sum of negativities of all the decomposed components. The convexity of the negativity guarantees that this decomposition shows the smallest negativity [33]. It is known that the separability criterion is satisfied in such cases of the "minimum decomposition" [34].

Based on this, the measure of entanglement defined as $E = -2\sum_i \lambda_i^-$ can be used [35], where λ_i^- are negative eigenvalues of the partial transpose of the density operator. Using Eqs. (5) and (6) and the aforementioned definition of the entanglement measure, the degree of entanglement for an odd ECS is obtained as

$$E_{\rm ECS}(\alpha,r) = -\frac{A+C-\sqrt{A^2+4B^2-2AC+C^2}}{4(-1+e^{4\alpha^2})}, \tag{8}$$

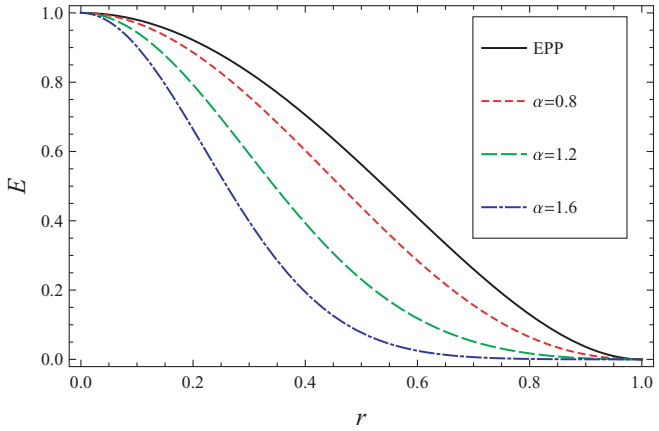

FIG. 1. (Color online) Degrees of entanglement E against the normalized time r. The EPP shows larger entanglement than ECSs at any time regardless of α.

and the degree of entanglement for the EPP is

$$E_{\mathrm{EPP}}(r) = (1 - r^2)^2. \tag{9}$$

We have plotted the degrees of entanglement for the EPPs and ECSs for several values of α in Fig. 1. As has been already discussed [35,36], the ECSs with large amplitudes decohere faster than those with small amplitudes. In the limit of $\alpha \to 0$, it is straightforward to show that

$$E_{\mathrm{ECS}}(\alpha,r) = -r^2 + \sqrt{1 - 2r^2 + 2r^4} < E_{\mathrm{EPP}}(r) \tag{10}$$

for $0 < r < 1$. Obviously, the EPP is always more entangled than the ECS for any values of α.

III. TELEPORTATION WITH ECS AND EPP

It is obvious that with quantum channels decohered for nonzero decay time, teleportation fidelities will degrade. This effect should not be neglected particularly for long-distance quantum teleportation. Detection inefficiency may be an even more crucial factor when considering practical quantum teleportation using optical systems. It is often considered as photon losses in front of ideal detectors. We also note that dark count rates may be non-negligible for the cases of highly efficient detectors such as photon-number-resolving detectors necessary for the teleportation using the ECS. In this section, we thoroughly analyze the first two degrading factors due to photon losses as depicted in Fig. 2.

A. Effects of channel decoherence

The fidelity F between input and output states for quantum teleportation is defined as $F = \langle\phi_{\mathrm{in}}|\rho_{\mathrm{out}}|\phi_{\mathrm{in}}\rangle$, where $|\phi_{\mathrm{in}}\rangle$ is the input state and ρ_{out} is the density operator of the output state. For the case of an ECS, one can use $|t\alpha\rangle$ and $|-t\alpha\rangle$ as a dynamic qubit basis in order to reflect amplitude losses as suggested in Ref. [10]. Then an unknown qubit reads

$$|\phi_{\mathrm{in}}\rangle = a|t\alpha\rangle + b|-t\alpha\rangle, \tag{11}$$

where a and b are arbitrary complex numbers under the normalization condition. The basis states $|t\alpha\rangle$ and $|-t\alpha\rangle$ are not orthogonal, but they approach such in the limit

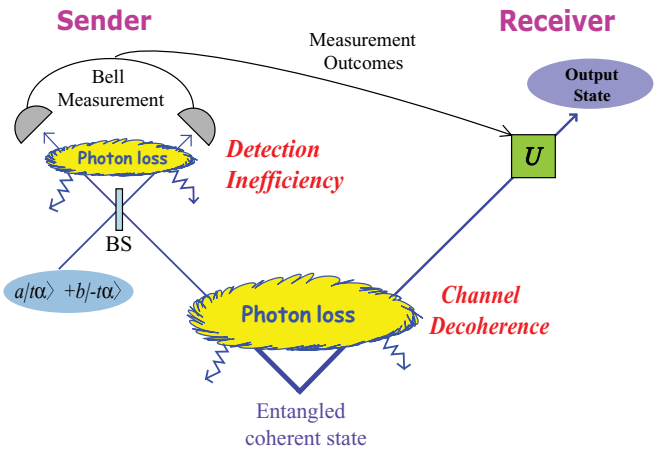

FIG. 2. (Color online) Teleportation protocol using the ECS with two kinds of "photon losses." Photon losses during the propagation of the quantum channel cause the "channel decoherence," while photon losses before ideal detectors are introduced to model detection inefficiency. BS represents a 50:50 beam splitter and U the unitary operation required to restore the input state.

for $t\alpha \gg 1$. One can construct an orthogonal basis, $|\pm\rangle = n_{\pm}(|t\alpha\rangle \pm |-t\alpha\rangle)$ with normalization factors $n_{\pm}$, using their linear superpositions [37]. In this way, one can consider the qubit (channel) in a two-dimensional ($2 \otimes 2$-dimensional) Hilbert space even under the decoherence effects. The input state can also be expressed as

$$|\phi_{\mathrm{in}}\rangle = \cos(u/2)e^{\frac{iv}{2}}|+\rangle + \sin(u/2)e^{-\frac{iv}{2}}|-\rangle. \tag{12}$$

The coefficient u and v are related to a and b as

$$\begin{aligned} a &= n_+ \cos(u/2)e^{\frac{iv}{2}} + n_- \sin(u/2)e^{-\frac{iv}{2}}, \\ b &= n_+ \cos(u/2)e^{\frac{iv}{2}} - n_- \sin(u/2)e^{-\frac{iv}{2}}. \end{aligned} \tag{13}$$

The initial total state is then represented as

$$\rho^{\mathrm{tot}} = |\phi_{\mathrm{in}}\rangle_A\langle\phi_{\mathrm{in}}| \otimes \{\rho_{\mathrm{ECS}}(\tau)\}_{BC}, \tag{14}$$

where A and B are modes for the sender while C for the receiver. In order to discriminate between the Bell states, a 50:50 beam splitter for modes A and B is used. We here define the beam-splitter operator as

$$U_{i,j}(\theta) = e^{-\frac{\theta}{2}(a_i^\dagger a_j - a_i a_j^\dagger)}, \tag{15}$$

where i and j are two field modes entering the beam splitter, and θ is related to the transmittivity $\zeta = \cos^2(\theta/2)$. The action of the 50:50 beam splitter, $U_{A,B}(\pi/2)$, may be characterized as $U_{A,B}(\pi/2)|\alpha\rangle_A|\beta\rangle_B = |(\alpha+\beta)/\sqrt{2}\rangle_A|(-\alpha+\beta)/\sqrt{2}\rangle_B$. The Bell states with coherent states in our context are

$$|\Phi^{\pm}\rangle = N_{\pm}(|t\alpha\rangle_1|t\alpha\rangle_2 \pm |-t\alpha\rangle_1|-t\alpha\rangle_2), \tag{16}$$

$$|\Psi^{\pm}\rangle = N_{\pm}(|t\alpha\rangle_1|-t\alpha\rangle_2 \pm |-t\alpha\rangle_1|t\alpha\rangle_2), \tag{17}$$

where $N_{\pm}$ are normalization factors. After the action of the beam splitter, two photon-number-resolving detectors are required for modes A and B to complete the Bell-state measurement [10]. The projection operators O_j for the

outcomes j representing the parity measurement can be written as

$$O_1 = \sum_{n=1}^{\infty} |2n\rangle_A\langle 2n| \otimes |0\rangle_B\langle 0|, \tag{18}$$

$$O_2 = \sum_{n=1}^{\infty} |2n-1\rangle_A\langle 2n-1| \otimes |0\rangle_B\langle 0|, \tag{19}$$

$$O_3 = \sum_{n=1}^{\infty} |0\rangle_A\langle 0| \otimes |2n\rangle_B\langle 2n|, \tag{20}$$

$$O_4 = \sum_{n=1}^{\infty} |0\rangle_A\langle 0| \otimes |2n-1\rangle_B\langle 2n-1|, \tag{21}$$

where we refer to Φ^+, Φ^-, Ψ^+, and Ψ^- as subscripts (or superscripts) 1, 2, 3, and 4 for simplicity. In addition to the operators in Eqs. (18)–(21), the error projection operator, $O_e = |0\rangle_A\langle 0| \otimes |0\rangle_B\langle 0|$, should also be considered because there is possibility for both the detectors not to register anything even though such probability is very small when α is reasonably large.

The un-normalized state after measurement outcome j is obtained as

$$\rho^j = \mathrm{Tr}_{AB}[U_{A,B}(\pi/2)\rho_{\mathrm{tot}}U^{\dagger}_{A,B}(\pi/2)O_j]. \tag{22}$$

Depending on the outcomes of the Bell-state measurement, different unitary rotations on the coherent-state qubit for mode C are required. Applying an appropriate unitary operation U_j, the unnormalized output state is obtained as $\rho^j_{\mathrm{out}} = U_j\rho^j U^{\dagger}_j$. While no transformation or only a simple phase shifter is required for the cases of Ψ^- and Φ^-, the displacement operator is required for the other two cases, which degrade the fidelity when α is small. We simply exclude such "fidelity-degrading" cases in this paper as the success probability with an ECS is always higher than that with an EPP even *without* those cases.

We find for the case of Ψ^-

$$\begin{aligned} p_4 f_4 &= \langle\phi_{\mathrm{in}}|\rho^4_{\mathrm{out}}|\phi_{\mathrm{in}}\rangle \\ &= (N^-_\alpha)^2 e^{-2t^2\alpha^2}\sinh(2t^2\alpha^2) \\ &\quad\times[|b|^2(a^*e^{-2t^2\alpha^2}+b^*)(ae^{-2t^2\alpha^2}+b) \\ &\quad+|a|^2(a^*+b^*e^{-2t^2\alpha^2})(a+be^{-2t^2\alpha^2}) \\ &\quad+e^{-4\alpha^2(1-t^2)}a^*b(a^*e^{-2t^2\alpha^2}+b^*)(a+be^{-2t^2\alpha^2}) \\ &\quad+e^{-4\alpha^2(1-t^2)}ab^*(a^*+b^*e^{-2t^2\alpha^2})(ae^{-2t^2\alpha^2}+b)] \\ &= p_2 f_2, \end{aligned} \tag{23}$$

where $p_j = \mathrm{Tr}(\rho^j_{\mathrm{out}})$ is the probability of measuring a particular outcome j and f_j is the teleportation fidelity with that outcome. The success probability p_4 for Φ_- is obtained as

$$\begin{aligned} p_4 &= \mathrm{Tr}(\rho^4_{\mathrm{out}}) \\ &= (N^-_\alpha)^2 e^{-2t^2\alpha^2}\sinh(2t^2\alpha^2)[|a|^2+|b|^2 \\ &\quad+e^{-4\alpha^2(1-t^2)}e^{-2t^2\alpha^2}(a^*b+ab^*)] \\ &= p_2. \end{aligned} \tag{24}$$

The same calculations can be performed for the case of Ψ_-, which results in the same fidelity and the success probability.

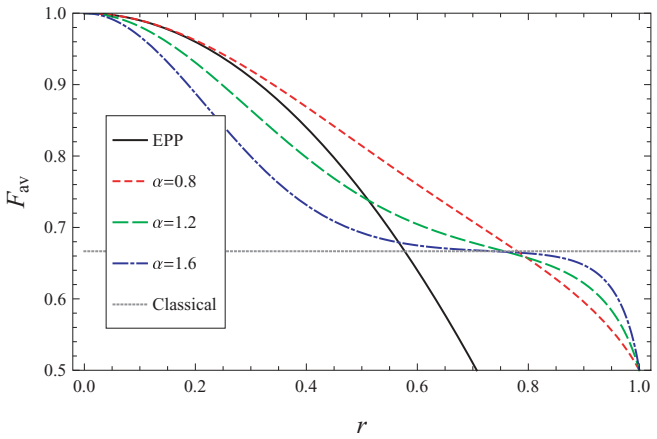

FIG. 3. (Color online) The average teleportation fidelities, F_{av}, of the ECSs and the EPPs as quantum channels against the normalized time r. The dotted horizontal line indicates the maximum classical limit, 2/3, which can be achieved by classical means.

The average teleportation fidelity over all unknown input states and the success probability are

$$F_{\mathrm{av}} = \frac{1}{4\pi}\int_0^{\pi}\sin u\,du\int_0^{2\pi}dv\frac{\sum_j p_j f_j}{\sum_j p_j}, \tag{25}$$

$$P = \frac{1}{4\pi}\int_0^{\pi}\sin u\,du\int_0^{2\pi}dv\sum_j p_j, \tag{26}$$

where the summations run over only 2 and 4 since we discard all the other cases. One can show by performing the integration in (26) that the average success probability for the ECS is $P_{\mathrm{ECS}} = 1/2$, regardless of α. As we perform the integration in (25), we obtain the expression

$$\begin{aligned} F_{\mathrm{ECS}}(\alpha,r) &= 2n\frac{l-m}{c} \\ &\quad+2n\frac{d^2(l-m)+2c^2m}{c^3}\frac{\mathrm{arctanh}\,d/c-d/c}{(d/c)^3}, \end{aligned} \tag{27}$$

where now $l = 3e^{8\alpha^2} - 5e^{4\alpha^2(r^2+1)} + 5e^{4\alpha^2(2+r^2)} - 3e^{4\alpha^2(1+2r^2)}$, $m = (e^{4\alpha^2}+e^{4r^2\alpha^2})(e^{4\alpha^2}-e^{4\alpha^2(1+r^2)})$, $n = e^{-4\alpha^2(1+r^2)}/16$, $c = e^{4\alpha^2}-1$, and $d = -e^{2(1+r^2)\alpha^2}+e^{-2(-1+r^2)\alpha^2}$. We have plotted the results in Fig. 3.

The calculations are straightforward for the case of the EPP because of the orthogonal nature of the qubit and the channel. In this case, only two ($|\Psi'^+\rangle$ and $|\Psi'^-\rangle$) among the four Bell states, $|\Phi'^{\pm}\rangle = (|H\rangle_1|H\rangle_2 \pm |V\rangle_1|V\rangle_2)/\sqrt{2}$ and $|\Psi'^{\pm}\rangle = (|H\rangle_1|V\rangle_2 \pm |V\rangle_1|H\rangle_2)/\sqrt{2}$, can be identified using linear optics elements and photodetectors. This means that the success probability cannot exceed 1/2 [6]. The average fidelity and the success probability can easily be obtained in the same manner explained earlier as $F_{\mathrm{EPP}}(r) = 1-r^2$ and $P_{\mathrm{EPP}} = (1-r^2)/2$, respectively. Here it is immediately clear that $P_{\mathrm{ECS}} = 1/2 > P_{\mathrm{EPP}}$: The success probability using the ECS is higher than that using the EPP regardless of α.

In Fig. 3, the average fidelities for the ECS and the EPP, F_{ECS} and F_{EPP}, respectively, are plotted and compared. The

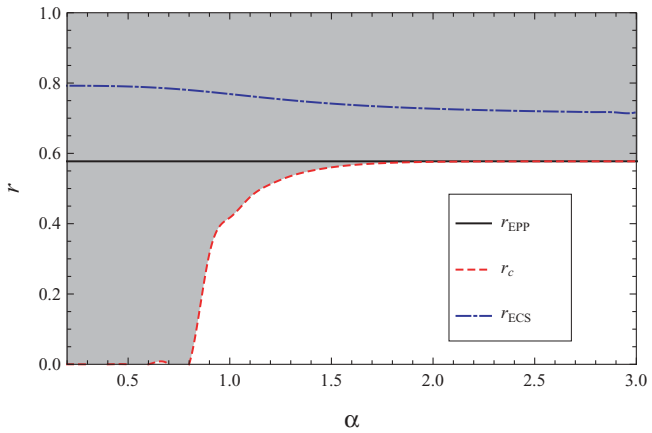

FIG. 4. (Color online) The average fidelity using the EPP falls below the classical limit at r_{EPP} (solid line). The average fidelity using the ECS, F_{ECS}, becomes larger than that using the EPP, F_{EPP}, at time r_c and falls below the classical limit at r_{ECS}. The gray-shaded area corresponds to $F_{ECS} > F_{EPP}$.

classical limit denoted by the horizontal dotted line in the figure is 2/3, under which quantum channels become useless for teleportation of qubits. We find that the teleportation fidelities using the ECSs stay above the classical limit longer than those with the EPP regardless of the values of α. As shown in Fig. 3, the EPP becomes useless for teleportation at time $r_{EPP} = 1/\sqrt{3} \approx 0.577$ while the ECSs become useless at r_{ECS}, where r_{ECS} is determined between 0.7 and 0.8, depending on α. We have investigated the cases for large values of α up to 4, and our numerical results lead us to conjecture that r_{ECS} converges to $\sim$0.7 when α becomes large. As shown in Fig. 4, F_{ECS} remains lower than F_{EPP} until the decoherence time r becomes r_c. When the decoherence time reaches r_c, F_{ECS} exceeds F_{EPP}. Of course, F_{ECS} eventually falls below the classical limit at time r_{ECS} as we mentioned earlier. Remarkably, $r_c \approx 0$ for $\alpha \lesssim 0.8$, which means that the ECSs outperform the EPP for these values of α.

Even though the EPP is always more entangled than the ECS (Fig. 1), it does not always mean higher teleportation fidelity (Fig. 3). The reason for this can be understood as originated from the different dynamics of the two channels under photon loss effects. With the ECS channels, we have been able to minimize the degradation of the teleportation fidelity using the dynamic qubit basis [10]. This is not possible with the EPP. Photon losses cause the EPP to have the "vacuum" elements both at the sender's mode and at receiver's. In other words, the decohered EPP gets out of the initial $2 \otimes 2$ Hilbert space composed of $|H\rangle$ and $|V\rangle$ and this "escape" for the EPP is a major difference from the case of the ECS. The vacuum portion at receiver's mode, C, results in a significant decrease of the teleportation fidelity. (On the contrary, in the following subsection, it becomes clear that the vacuum elements at sender's modes, A and B, are noticed by a failure of the Bell-state measurement and such an error can be discarded so that the fidelity is not affected.)

We here comment on the difference between the previous result in Ref. [10] and ours in this paper. In Ref. [10], the time r at which the teleportation fidelity of the ECS falls below the classical limit was independent of α. In that paper, the singlet fraction of the channel state was used to calculate the optimal teleportation fidelity using the method suggested in Ref. [38]. However, this method is not optimized for the ECS under our decoherence model based on photon losses: When ρ^{-}_{ECS} is partially traced over one of the modes, the reduced density matrix is not proportional to the identity matrix, which is the condition required to apply the singlet fraction method presented in Ref. [38].

So far, we have not considered the even ECS. For the same reason as the case of the odd ECS, only ψ^+ and ϕ^+ can be considered the successful Bell measurement results. For the results with the even ECS, the teleportation fidelity becomes identical to the case of the odd ECS. However, the success probability is lower than that of the odd ECS, according to our calculation for the same value of α. The reason for this is as follows. We utilize the results of odd photon detection for the case of the odd ECS, while the results of the nonzero even photon detection, corresponding to ψ^+ and ϕ^+, are used for the case of the even ECS. The odd photon detection probability is the same as the even photon detection probability when taking the average over all input states. However, the even photon detection probability contains the "all-zero" cases, which are eventually discarded, and this inconclusive failure probability gets larger as the amplitude becomes smaller. Therefore, the even ECS channel results in lower success probability unless $\alpha \to \infty$.

B. Effects of detection inefficiency

We now consider the inefficiency of detectors that is one of the major obstacles to the realization of quantum teleportation using optical systems. An inefficient detector can be modeled by inserting a beam splitter of transmittivity η in front of the perfect detector, where the beam splitter operation mixing the light with fictitious vacuum mode can be denoted as $U^{\eta}_{i,j} \equiv U_{i,j}(\theta_\eta)$, where $\theta_\eta = 2\cos^{-1}\sqrt{\eta}$, where i and j are indices for modes. In order to perform the Bell-state measurement, we first need to apply the 50:50 beam splitter to the total density operator ρ^{tot} in Eq. (14). The beam-splitter operations, U^{η}, for inefficient detectors are then applied to incorporate detection inefficiency. The resultant density operator after tracing out the irrelevant vacuum modes (v_1 and v_2) is

$$(\rho^{\eta})_{ABC} = \mathrm{Tr}_{v_1,v_2}\big[U^{\eta}_{A,v_1}U^{\eta}_{B,v_2}U_{A,B}(\pi/2)\{(\rho^{tot})_{ABC} \otimes (|0\rangle\langle 0|)_{v_1} \otimes (|0\rangle\langle 0|)_{v_2}\}U^{\dagger}_{A,B}(\pi/2)U^{\eta\dagger}_{B,v_2}U^{\eta\dagger}_{A,v_1}\big]. \tag{28}$$

The un-normalized density matrix for measurement outcome j is given as $\rho^{j}_{out} = U_j[\mathrm{Tr}_{AB}(\rho^{\eta}O_j)]U^{\dagger}_j$. Using Eqs. (18) and (19), we find

$$p_2 f_2 = p_4 f_4 = \langle\psi_{in}|\rho^4_{out}|\psi_{in}\rangle = D(N^-_\alpha)^2[|L|^2 + |M|^2 + 2e^{-4\alpha^2 r^2}C^2\,\mathrm{Re}(M^*L)], \tag{29}$$

$$p_2 = p_4 = \mathrm{Tr}\big(\rho^4_{out}\big) = D(N^-_\alpha)^2[|a|^2 + |b|^2 + 2e^{-2\alpha^2(1+r^2)}C^2\mathrm{Re}(a^*b)], \tag{30}$$

where $D = e^{-2\eta(1-r^2)\alpha^2}\sinh[2\eta(1-r^2)\alpha^2]$, $C = e^{-2(1-r^2)\alpha^2(1-\eta)}$, $M = a^*(a + be^{-2(1-r^2)\alpha^2})$, and $L = b^*(ae^{-2(1-r^2)\alpha^2} + b)$, and

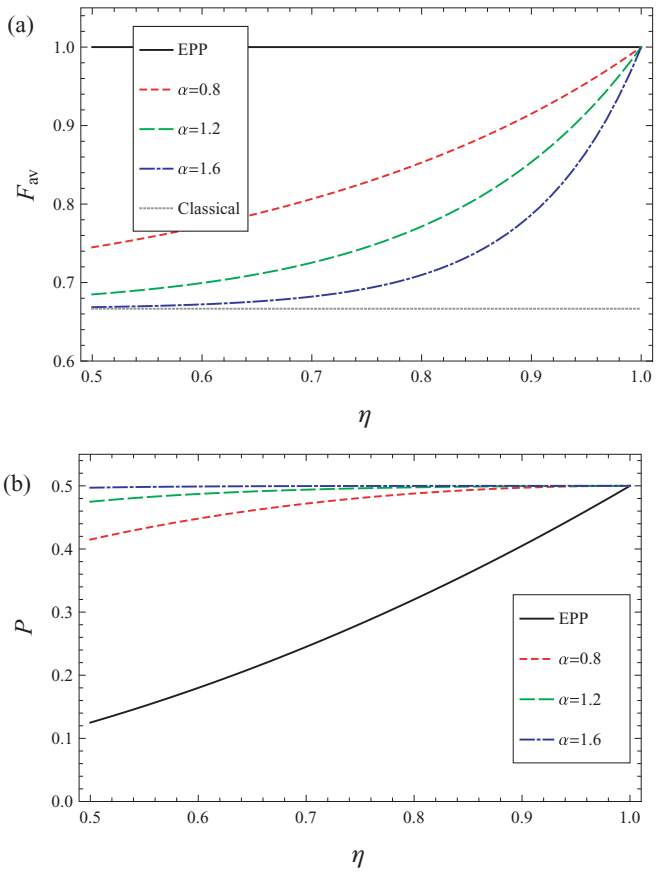

FIG. 5. (Color online) (a) Teleportation fidelities using the ECS and the EPP as quantum channels in terms of the efficiency η of detectors. The ECS with large α shows smaller fidelity than that with small α while the fidelity using the EPP is not affected η. (b) The success probabilites of teleportation using the ECS and EPP. The success probability of the EPP decreases faster than that of the ECS by η. Decoherence of the channels is not considered to clearly see the effect of the detection inefficiency.

the average fidelity is obtained using Eq. (25) as

$$F_{\mathrm{ECS}}(\eta,\alpha,r) = 2n\frac{l-m}{c} + 2n\frac{d^2(l-m)+2c^2m}{c^3}\frac{\operatorname{arctanh} d/c - d/c}{(d/c)^3}, \tag{31}$$

where now $l = 3S^{2(1+\eta)} - 5S^{2(r^2+\eta)} + 5S^{2(2+r^2\eta)} - 3S^{2[1+r^2(1+\eta)]}$, $m = (S^2+S^{2r^2})(S^{2\eta}-S^{2(1+r^2\eta)})$, $n = S^{-2(1+r^2\eta)}/16$, $c = S^2 - S^{-2(-1+r^2)(-1+\eta)}$, $d = -S^{(1+r^2)} + S^{-(-1+r^2)(-1+2\eta)}$, and $S = e^{-2\alpha^2}$.

We first plot the teleportation fidelities for $r = 0$ (i.e., without decoherence) in Fig. 5. It is clear that the ECSs with larger amplitudes are more sensitive to inefficiency of the detectors (i.e., decrease of η). The reason for this is similar to the case of the channel decoherence. The action of the beam splitter used for the Bell-state measurement may be described as

$$\begin{aligned}(a|\alpha\rangle + b|-\alpha\rangle)|\alpha\rangle &\rightarrow a|\sqrt{2}\alpha\rangle|0\rangle + b|0\rangle|\sqrt{2}\alpha\rangle,\\ (a|\alpha\rangle + b|-\alpha\rangle)|-\alpha\rangle &\rightarrow a|0\rangle|-\sqrt{2}\alpha\rangle + b|-\sqrt{2}\alpha\rangle|0\rangle.\end{aligned} \tag{32}$$

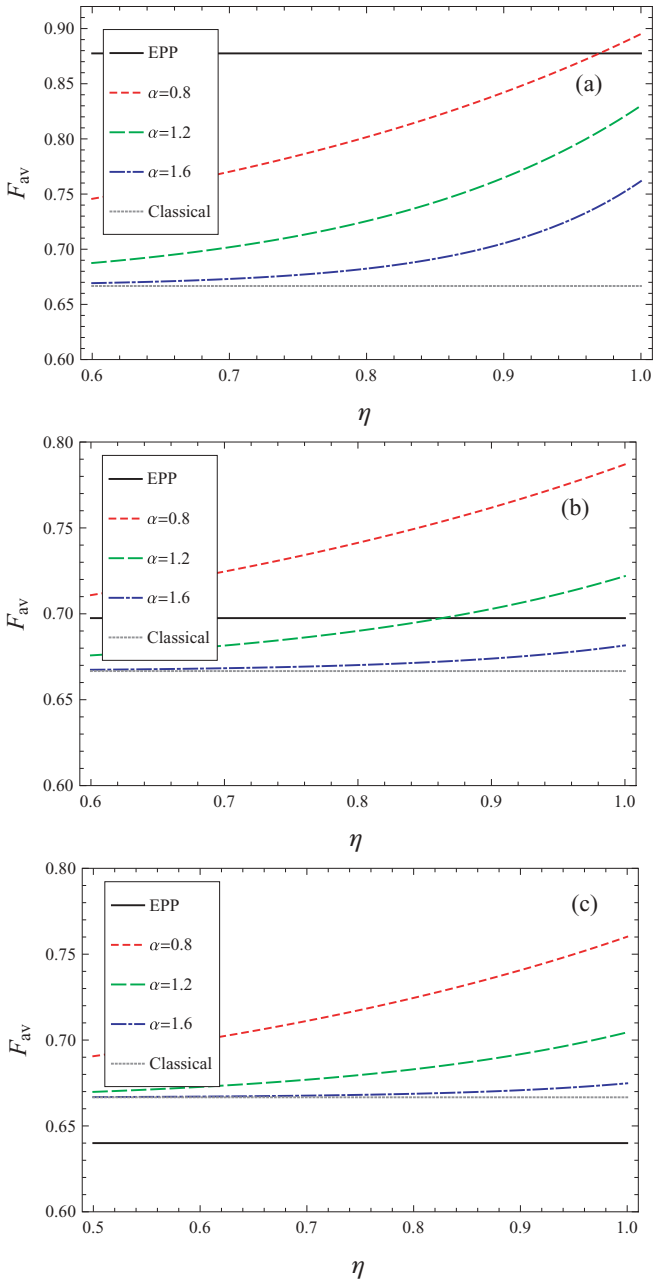

FIG. 6. (Color online) Teleportation fidelities against detection efficiency η at decoherence time (a) $r = 0.35$, (b) $r = 0.55$, and (c) $r = 0.6$ for several values of α. As r becomes larger, the fidelity with the EPP drops more rapidly than the fidelities with the ECS.

It is then obvious that there are, for example, "cross" terms such as $|\pm\sqrt{2}\alpha\rangle\langle\mp\sqrt{2}\alpha|$, as well as the "diagonal" terms such as $|\pm\sqrt{2}\alpha\rangle\langle\pm\sqrt{2}\alpha|$, before the detection. Then the cross terms described earlier in the density matrix are reduced as $\propto e^{-4(1-\eta)\alpha^2}|\pm\sqrt{\eta}\sqrt{2}\alpha\rangle\langle\mp\sqrt{\eta}\sqrt{2}\alpha|$, while the diagonal terms change simply to $\propto|\sqrt{\eta}\sqrt{2}\alpha\rangle\langle\sqrt{\eta}\sqrt{2}\alpha|$ due to photon losses modeled by beam splitters right in front of the "perfect" detectors. It is then straightforward to see that this reduction of the cross terms eventually causes the teleported qubit to be mixed. Therefore, the inefficiency of the detectors (modeled by the additional beam splitters) causes the teleported qubit to be "more mixed" when the amplitude is larger.

On the contrary, the detection efficiency does not affect the teleportation fidelity using the EPP. In this case, the number of photons that should be registered by the Bell measurement is precisely defined as two. The Bell measurement succeeds only when two photons are registered by two of the four detectors used for the measurement [6]. If photon loss occurs due to the inefficiency of the detectors so that only one photon (or no photon at all) is detected, it will be immediately recognized by Alice as a failure. Alice can then simply filter out this kind of "detected" error to prevent the decrease of the fidelity.

The success probability of teleportation using the ECS is obtained by Eq. (26), p_2, and p_4 in Eq. (30) as

$$P_{\mathrm{ECS}}(\eta,\alpha,r) = \tfrac{1}{4}S^{-2(-1+r^2)(-1+\eta)}(-1+S^{2(-1+r^2)\eta}) \times (-1+S^{2[1+(-1+r^2)(-1+\eta)]})(-1+S^2)^{-1} \times (-1+S^{2(-1+r^2)})^{-1}. \quad (33)$$

The ECSs with small α show lower success probabilities than large α, as seen in Fig. 5(b). When α is small, even a small amount of photon losses may significantly increase the possibility of O_e (i.e., silence of both the detectors), while this is not the case for large α. Therefore, the success probability using the ECSs with small α is more sensitive to detection inefficiency, which is opposite to the case of the fidelity.

Of course, the "filtering out" of the detected errors for the case of the EPP results in the more rapid decrease of the success probability. The success probability using the EPP including the inefficient detector is similarly obtained as for the case of the ECS as

$$P_{\mathrm{EPP}}(\eta,r) = \frac{1-r^2}{2}\eta^2 \quad (34)$$

and is plotted in Fig. 5(b). The additional factor η^2 when compared to the probability for the perfect detection case means that each of the two photons in the Bell-measurement module is successfully detected with probability η. Here we can easily check that the success probability of the ECS is larger than the EPP regardless of α, r, and η. Equation (33) is reduced to $[2\eta + r^2(-1+\eta)\eta - \eta^2]/2$ when $\alpha \to 0$ and cannot be smaller than $P_{\mathrm{EPP}}(\eta,r)$ for any η and r.

C. Photon losses both in channels and at detectors

So far, we have separately considered two different kinds of photon losses, the losses in the channel (referred to as channel decoherence) and the losses at the detectors (detection inefficiency) used for the Bell-state measurements. In realistic situations, both kinds of losses exist, and it is meaningful to know how the fidelities change under the combination of these effects.

If the ECS shows larger fidelity than the EPP with the perfect detector, it is expected that this is true with imperfect detectors for some moderate values of η. As shown in several examples in Fig. 6, the ECSs begin to show larger fidelities even with inefficient detectors as the decoherence time gets larger. As noted in the previous section, only the channel decoherence degrades the teleportation fidelity with the EPP, while the teleportation fidelity with the ECS is affected by both the channel decoherence and the detection inefficiency. When the decoherence effect is as dominant as $r > 0.577$, the teleportation fidelity with EPP becomes lower than the classical limit, $2/3$, and the teleportation fidelities with the ECSs are always higher regardless of any other conditions.

IV. CONCLUSIONS

In this paper, our attempt was to compare ECSs and EPPs as resources for QIP under realistic conditions. We have considered decoherence caused by photon losses in ECSs and EPPs as quantum channels for teleportation. We have pointed out that entanglement of the EPPs is always larger than that of the ECSs in a dissipative environment. On the other hand, the ECSs outperform the EPPs for the standard teleportation protocol in fidelities for $\alpha \lesssim 0.8$. Furthermore, the success probabilities for teleportation using the ECSs are always higher than those using the EPPs. However, as α gets larger, the range for which the EPPs show higher fidelities appears.

In general, teleportation fidelity using the ECSs remains over the classical limit longer than that of the EPPs. In other words, even when the EPPs become useless for teleportation due to significant decoherence effects, the ECSs can still be useful for the same purpose. Based on our numerical results we would conjecture that the ECSs are useful for teleportation until the normalized time becomes $r \approx 0.7$ regardless of α while the EPPs become useless when $r \approx 0.577$. However, when α is too large as, for example, $\alpha > 1.6$, this fidelity merit of the ECSs is too tiny so as to make the teleportation process useless. We have thus pointed out that the degrees of decoherence in the quantum channels are a crucial factor to decide whether the ECSs or the EPPs should be used for efficient QIP. On the other hand, it should be noted that the requirement for fault-tolerant quantum computing using coherent-state qubits is very demanding [17].

We also pay special attention to detection inefficiency that is a crucial detrimental factor in realizing practical QIP using all-optical systems. We point out that when inefficient detectors are used for Bell-state measurements, the teleportation scheme using the ECSs suffers undetected errors that result in the degradation of fidelity. This is not the case for the teleportation scheme using the EPPs as photon losses right before the detector are noticed by the absence of the detection signals itself. Finally, we have presented analytical results and examples when both the channel decoherence and the detection inefficiency are considered. Our results based on a thorough quantitative analysis reveal the merits and demerits of the two types of entangled states in realizing practical QIP under realistic conditions and provide useful guidelines for the choice among the well-known QIP schemes based on optical systems.

ACKNOWLEDGMENTS

The authors thank Chang-Woo Lee for useful discussions. This CRI work was supported by a National Research Foundation of Korea (NRF) grant funded by the Korea government (MEST) (Grant No. 3348-20100018), Center for Subwavelength Optics (R11-2008-095-01000-0), and the World Class University (WCU) program. H.J. acknowledges support from TJ Park foundation.

[1] P. Kok, W. J. Munro, K. Nemoto, T. C. Ralph, J. P. Dowling, and G. J. Milburn, Rev. Mod. Phys. **79**, 135 (2007).

[2] T. C. Ralph and G. J. Pryde, Prog. Opt. **54**, 209 (2009).

[3] E. Knill, R. Laflamme, and G. J. Milburn, Nature (London) **409**, 46 (2001).

[4] D. Gottesman and I. L. Chuang, Nature (London) **402**, 390 (1999).

[5] L. Vaidman and N. Yoran, Phys. Rev. A **59**, 116 (1999).

[6] N. Lütkenhaus, J. Calsamiglia, and K.-A. Suominen, Phys. Rev. A **59**, 3295 (1999).

[7] D. Bouwmeester, J.-W. Pan, K. Mattle, M. Eibl, H. Weinfurter, and A. Zeilinger, Nature (London) **390**, 575 (1997).

[8] J. Calsimiglia and N. Lütkenhaus, Appl. Phys. B **72**, 67 (2001).

[9] S. J. van Enk and O. Hirota, Phys. Rev. A **64**, 022313 (2001).

[10] H. Jeong, M. S. Kim, and J. Lee, Phys. Rev. A **64**, 052308 (2001).

[11] D. Wilson, H. Jeong, and M. S. Kim, J. Mod. Opt. **49**, 851 (2002); H. Jeong and N. Ba An, Phys. Rev. A **74**, 022104 (2006); H. Jeong, W. Son, M. S. Kim, D. Ahn, and C. Brukner, *ibid.* **67**, 012106 (2003); M. Stobinska, H. Jeong, and T. C. Ralph, *ibid.* **75**, 052105 (2007); H. Jeong, *ibid.* **78**, 042101 (2008); C.-W. Lee and H. Jeong, *ibid.* **80**, 052105 (2009); H. Jeong, M. Paternostro, and T. C. Ralph, Phys. Rev. Lett. **102**, 060403 (2009); M. Paternostro and H. Jeong, Phys. Rev. A **81**, 032115 (2010).

[12] X. Wang, Phys. Rev. A **64**, 022302 (2001).

[13] H. Jeong and M. S. Kim, Phys. Rev. A **65**, 042305 (2002).

[14] H. Jeong and M. S. Kim, Quantum Inf. Comput. **2**, 208 (2002).

[15] T. C. Ralph, A. Gilchrist, G. J. Milburn, W. J. Munro, and S. Glancy, Phys. Rev. A **68**, 042319 (2003).

[16] N. Ba An, Phys. Rev. A **68**, 022321 (2003).

[17] A. P. Lund, T. C. Ralph, and H. L. Haselgrove, Phys. Rev. Lett. **100**, 030503 (2008).

[18] N. Ba An, Phys. Lett. A **373**, 1701 (2009).

[19] P. Marek and J. Fiurášek, Phys. Rev. A **82**, 014304 (2010).

[20] W. P. Schleich, *Quantum Optics in Phase Space* (Wiley-VCH, Berlin, 2001).

[21] C. L. Salter, R. M. Stevenson, I. Farrer, C. A. Nicoll, D. A. Ritchie, and A. J. Shields, Nature (London) **465**, 594 (2010).

[22] A. Ourjoumtsev, H. Jeong, R. Tualle-Brouri, and P. Grangier, Nature (London) **448**, 784 (2007).

[23] H. Takahashi, K. Wakui, S. Suzuki, M. Takeoka, K. Hayasaka, A. Furusawa, and M. Sasaki, Phys. Rev. Lett. **101**, 233605 (2008).

[24] T. Gerrits, S. Glancy, T. S. Clement, B. Calkins, A. E. Lita, A. J. Miller, A. L. Migdall, S. W. Nam, R. P. Mirin, and E. Knill, Phys. Rev. A **82**, 031802 (2010).

[25] A. P. Lund, H. Jeong, T. C. Ralph, and M. S. Kim, Phys. Rev. A **70**, 020101(R) (2004); P. Marek, H. Jeong, and M. S. Kim, *ibid.* **78**, 063811 (2008).

[26] J. S. Neergaard-Nielsen, M. Takeuchi, K. Wakui, H. Takahashi, K. Hayasaka, M. Takeoka, and M. Sasaki, Phys. Rev. Lett. **105**, 053602 (2010).

[27] E. A. Dauler, A. J. Kerman, and B. S. Robinson, J. Mod. Opt. **56**, 364 (2009).

[28] R. Hadfield, Nat. Photon. **3**, 696 (2009).

[29] B. C. Sanders, Phys. Rev. A **45**, 6811 (1992).

[30] S. J. D. Phoenix, Phys. Rev. A **41**, 5132 (1990).

[31] A. Peres, Phys. Rev. Lett. **77**, 1413 (1996).

[32] M. Horodecki, P. Horodecki, and R. Horodecki, Phys. Lett. A **223**, 1 (1996).

[33] G. Vidal and R. F. Werner, Phys. Rev. A **65**, 032314 (2002).

[34] S. Lee, D. P. Chi, S. D. Oh, and J. Kim, Phys. Rev. A **68**, 062304 (2003).

[35] J. Lee, M. S. Kim, Y.-J. Park, and S. Lee, J. Mod. Opt. **47**, 2151 (2000).

[36] M. S. Kim and V. Bužek, Phys. Rev. A **46**, 4239 (1992).

[37] A direct comparison between arbitrary polarization qubits, $\mu|H\rangle + \nu|V\rangle$, and coherent-state qubits, $\mu|\alpha\rangle + \nu|-\alpha\rangle$, is not straightforward when α is small due to the nonzero overlap between the two component coherent states. It should be noted that we use the orthogonal basis, $|+\rangle$ and $|-\rangle$, for coherent-state qubits in order to calculate the average fidelity for a "fair comparison" with the polarization-qubit case. In this sense, the input coherent-state qubit in comparison to the polarization qubit, $\mu|H\rangle + \nu|V\rangle$, should be considered to be $\mu|+\rangle + \nu|-\rangle$, rather than $\mu|\alpha\rangle + \nu|-\alpha\rangle$, when the overlap $|\langle\alpha|-\alpha\rangle|^2$ is non-negligible.

[38] M. Horodecki, P. Horodecki, and R. Horodecki, Phys. Rev. A **60**, 1888 (1999).